

PROBE TACK TESTS OF PRESSURE-SENSITIVE ADHESIVES WITH FLAT AND SPHERICAL PUNCHES

KENNETH R. SHULL
ALFRED J. CROSBY

Department of Materials Science
Northwestern University

HAMED LAKROUT
COSTANTINO CRETON

Lab. Physico-Chimie Structurale
et Macromoleculaire ESPCI
Paris, France

INTRODUCTION

Axisymmetric adhesion tests using either flat or spherical punches have played a very important role in understanding the fundamental mechanisms of adhesion. For example, the geometry of a spherical punch pressing against a flat substrate has been used in fundamental studies of the tackiness of crosslinked elastomers.[1-4](Figure 1a) In this geometry relationships between the contact force (P), contact radius (a), and displacement (δ) can be used to measure the adhesive forces between the sphere and flat adhesive layer.[4] With this characterization method, accurate measurements the relationship between the energy release rate (G) and the crack velocity (v) can be made.

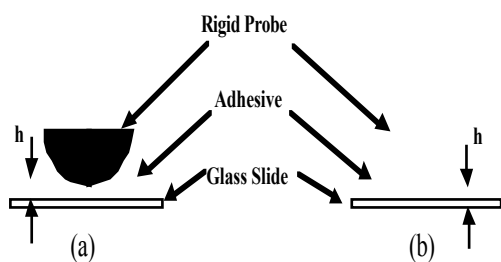


Figure 1 (a) Spherical punch geometry. (b) Flat punch geometry.

Flat punch tests (Figure 1b) have often been the choice of industrial research labs and quality control applications, and are the basis for a commonly used ASTM standard.[5] More recently, the practice of collecting the entire stress-strain curve from the bonding/debonding process has added value to the flat punch geometry by making its sensitivity more quantifiable[6-8]. Specific applications of the flat

punch (Creton *et al.*) and of the spherical punch (Shull *et al.*) from our own work are given elsewhere in these proceedings. Our purpose here is to compare results obtained from both types of tests, and illustrate the complementary nature of these methods.

COMPARISON OF SPHERICAL AND FLAT PUNCH GEOMETRIES

In the spherical geometry, the contact area decreases but often remains circular during the debonding process. The perimeter of the contact zone in this case can be viewed as a propagating crack which moves toward the center of the contact zone. Because the experimental geometry in this case is well controlled, the driving force for crack propagation can be obtained quantitatively (at least for elastic systems) and related to the resultant crack velocity.[4] An important point in these experiments is that the curvature of the rigid punch limits the contact radius to values which are generally less than about five times the thickness of the adhesive layer ($a/h < 5$). For a flat punch the contact radius of the punch is defined by the size of the punch itself. With proper alignment of the punch, values of a/h as large as 100 can be obtained. When the flat punch is pulled away from the adhesive layer, the contact area remains constant until cavities form at the punch/adhesive interface. These voids grow rapidly to an equilibrium size at which point the loading energy is used to extend an array of fibrils. In most commercial PSA's, this fibril drawing process is responsible for the high adhesion energies that are typically measured. The entire debonding sequence for the flat geometry is illustrated schematically in Figure 4.

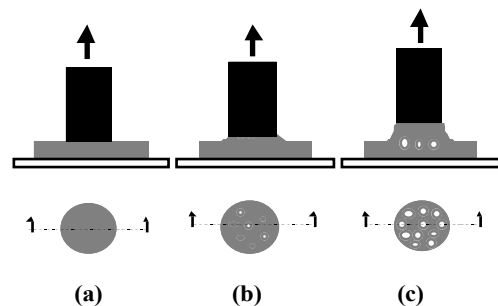


Figure 2 Typical debonding process for flat punch.

The primary difference between the two geometries is the nature of the stress state under the punch. For the spherical punches with low values of a/h , the behavior is dominated by the stress singularity at the edge of the contact zone. In other words, if no other significant defects on the interface are present, the most energetically favorable debonding mode is crack propagation from the contact perimeter. For the large values of a/h characteristic of the flat probe geometry, the stress singularity near the edge is also present, but is greatly reduced in importance. In these cases, the hydrostatic stress within the adhesive is large

enough to lead to nucleation and growth of voids, while the driving force for debonding to occur from the edge of the contact zone is very small.[8]

FRACTURE MECHANICS FORMULATION

Given this qualitative understanding of the mechanisms governing the debonding behavior for both geometries, we can begin to formulate a relationship between the adhesive's behavior in the two tests. As is generally the case, we will assume that the relationship between the crack driving force (energy release rate), \mathcal{G} , and the crack tip velocity, v , is a material property.[4, 9-12] In other words, if the adhesive and substrate materials are the same for both test geometries, then the same relationship will exist between \mathcal{G} and v . The primary advantage of the spherical probe geometry is that the $\mathcal{G}(v)$ relationship can be determined quantitatively, at least for an adhesive with substantial elastic character. The existence of a circular contact zone allows us not only to measure the crack velocity easily, but also to use a simple fracture mechanics approach to calculate \mathcal{G} at any point during the debonding process. This approach has been used successfully and verified by several groups.[1, 4]

Qualitatively, the debonding mechanisms for both types of tests are controlled by energetic considerations. As the punch is pulled away from the adhesive, mechanical energy is stored in the adhesive material as it is deformed. The energy release rate quantifies the amount of energy which is recovered when an incremental area of the adhesive detaches from the punch. Part of this energy is stored as surface energy in the new surfaces which are created, but most of it is dissipated irreversibly within the adhesive in a region near the crack tip. Although this sequence of events is easier to visualize for a uniform crack, the overall debonding process is still controlled by the same energy balance for a flat punch test where cavitation typically occurs. Consider the sequence of events in Figure 2. In order for an annular ring with an area of dA to debond from the outer most region of contact, a certain amount of energy is required. For large values of a/h , the available elastic energy ($\mathcal{G}dA$) is simply too low. In this case significant hydrostatic stresses develop within the contact region, leading to the nucleation and growth of cavities.[13]

The question of whether cavitation or crack propagation from the edge will occur can be determined by considering the data plotted in Figure 3. In this figure, the energy release rate for inward growth of a crack from the edge of contact is plotted against the average stress ($(\sigma_{avg} = -P/\pi a^2)$) for a spherical punch ($a/h \approx 5$) and for flat punch ($a/h \approx 100$). These values for \mathcal{G} are obtained from the following general equation, valid for a linearly elastic material:

$$\mathcal{G} = -\frac{a-P}{4\pi a} \frac{dC}{da} \quad (1)$$

Here a is the contact radius, P is the applied load (negative when in tension), P' is the load corresponding to a given

contact radius in the absence of adhesive interactions, and C is the compliance of the adhesive layer. As the thickness of the adhesive layer decreases, its compliance decreases as well, as does its derivative and the resultant driving force for crack propagation.

For a flat punch, $P' = 0$, and the energy release rate is obtained directly from the compliance expression. The data in Figure 3 are obtained by differentiating an analytic form of the compliance[4] determined from asymptotic limits and the numerical finite element data of Ganghoffer and Gent.[14] For very large values of a/h , the compliance of the adhesive layer is inversely proportional to the bulk modulus of the material. For smaller values of a/h , deviations from the incompressible limit are much less important. Experimentally, cavitation is observed for values of the average tensile stress that are comparable to Young's modulus for the elastic layer ($\sigma_{avg}/E \approx 1$). A critical value of \mathcal{G} , referred to here as \mathcal{G}_0 , must be exceeded in order for a finite crack velocity to be observed. The minimum possible value of \mathcal{G}_0 is the thermodynamic work of adhesion, which is typically of the order of 0.05 J/m^2 for polymeric systems. For $a/h = 70$, even this relatively low value of \mathcal{G} is not exceeded for $\sigma_{avg}/E = 1$, indicating that cavitation in the interior of the contact zone will precede crack propagation from the edge of the contact zone. For the spherical punch, large \mathcal{G} values are reached before significant stresses can develop within the adhesive. In this case debonding proceeds by from the outside of the contact zone, with no observed cavitation.

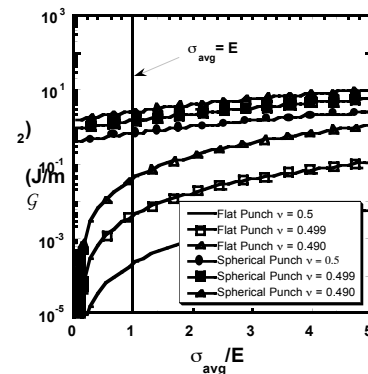


Figure 3: Energy release rate for spherical and flat punch tests as a function of average stress, for adhesives with $E = 10^4 \text{ Pa}$. For the spherical punch, $a/h = 4.86$, $h = 121 \text{ }\mu\text{m}$ and R (punch radius of curvature) = 4.0 mm . For the flat punch, $a/h = 70.4$ and $h = 71 \text{ }\mu\text{m}$.

For the spherical punch P' is non-zero, and a positive crack driving force is obtained even when $\sigma_{avg} = 0$. In this case compressive forces in the middle of the contact zone are offset by tensile forces at the edges.

CAVITY GROWTH

As shown in Figure 4 a cavitated surface resembles an array of individual adhesion tests which are coupled to one another. In this case the distance between cavities is determined by the relaxation of stored energy in the system. Figure 5 illustrates the experimentally determined spacing between two cavities for an acrylic adhesive with $a/h = 70$. The distance between cavities decreases over time until an equilibrium distance is established. This point corresponds to a crack velocity of zero; where \mathcal{G} is equal to or less than \mathcal{G}_0 . While $\mathcal{G} < \mathcal{G}_0$, interfacial failure will be delayed and fibril extension will ensue (Figure 5c) until the stored energy in the fibrils causes $\mathcal{G} > \mathcal{G}_0$ and final detachment occurs. The actual value of \mathcal{G} which is being applied to the cracks defining the perimeter of a void is a complicated function of the geometry. Our hypothesis at this point is that the relationship between this value of \mathcal{G} and the relevant crack velocity is the same as the relationship between \mathcal{G} and v that is more directly obtained by using a spherical punch. An advantage of the flat punch geometry is that the balance between fibrillation and cavity growth that determines the observed stress/strain behavior can be very sensitive to the $\mathcal{G}(v)$ expression.

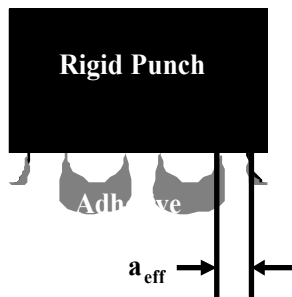


Figure 4: Schematic of cavitated flat punch interface.

SUMMARY

A qualitative picture of the relationships between adhesion experiments conducted with flat and spherical punches has been developed. By using a spherical punch with a relatively low value of a/h (ratio of the contact radius to the adhesive layer thickness) one can maintain a well-defined geometry during the debonding process, allowing one to quantify the relationship between the crack driving force, \mathcal{G} , and the resultant crack velocity. This $\mathcal{G}(v)$ relationship governs the debonding process in any test or practical situation.

By using a properly aligned flat punch, one can access much larger values of a/h , where cavitation throughout the contact zone precedes crack growth originating from the outer periphery of the contact zone. In this the balance between cavity growth and fibril extension can be very sensitive to the details of the $\mathcal{G}(v)$ relationship. For this reason, differences between systems which are difficult to observe when using a spherical punch can sometimes be readily observed when using a flat punch.

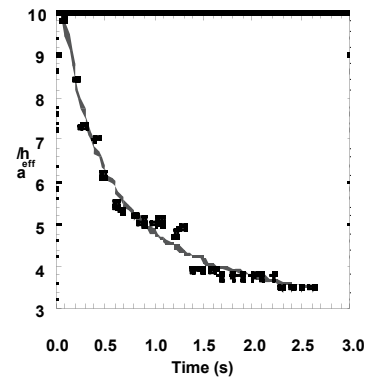


Figure 5 Time dependence of the distance between cavities (a_{eff}) normalized by the layer thickness (h) for flat punch test on a commercial acrylic adhesive with $a/h = 70$.

ACKNOWLEDGEMENTS

Work at Northwestern University was sponsored by the National Science Foundation under Grant NSF DMR-9457923. The collaborative work described here was supported by the NSF US-France Cooperative Science Program.

REFERENCES

1. M. Barquins and D. Maugis, *J. Adhesion* **13**, 53 (1981).
2. D. Ahn and K.R. Shull, *Macromolecules* **29**, 4381 (1996).
3. K.L. Johnson, K. Kendall and A.D. Roberts, *Proc. R. Soc. Lond. A* **324**, 301 (1971).
4. K.R. Shull, D. Ahn, W.-L. Chen, C.M. Flanigan and A.J. Crosby, *Macromol. Chem. Phys.* **199**, 489 (1998).
5. *Annual Book of ASTM Standards* **15.06**, 180 (1996).
6. A. Zosel, *Coll. Polym. Sci.* **263**, 541 (1985).
7. C. Creton, *Materials Science and Technology : A Comprehensive Treatment* **18**, 708 (1997).
8. H. Lakrout, P. Sergot and C. Creton, *J. Adhesion*, In press
9. A.N. Gent and J. Schultz, *Journal of Adhesion* **3**, (1972).
10. H. Chun and A.N. Gent, *J. Polym. Sci., Part B: Polym. Phys.* **34**, 2223 (1996).
11. E.H. Andrews and A.J. Kinloch, *J. Polym. Sci., Polym. Symp.* **46**, 1 (1974).
12. D. Maugis and M. Barquins, *J. Phys. D: Appl. Phys.* **11**, 1989 (1978).
13. A.N. Gent and C. Wang, *Journal of Materials Science* **26**, 3392 (1991).
14. J.F. Ganghoffer and A.N. Gent, *J. Adhesion* **48**, 75 (1995).